U.S. ARMY COMBAT CAPABILITIES DEVELOPMENT COMMAND
CHEMICAL BIOLOGICAL CENTER
ABERDEEN PROVING GROUND, MD 21010-5424

DEVCOM CBC-TR-1782

Purification and Characterization of a Membrane Sculpting Bacterial BAR Domain-Containing Protein for Engineering Tunable Scaffolds into Novel Biological Metamaterials

Daniel A. Phillips

OAK RIDGE INSTITUTE FOR SCIENCE AND EDUCATION
Oak Ridge, TN 37830-8007

Aleksandr E. Miklos
Patricia E. Buckley

RESEARCH & TECHNOLOGY DIRECTORATE
APG, MD 21010-5424

Jennifer A. Lee
DEFENSE THREAT REDUCTION AGENCY
Fort Belvoir, VA 22060-6201

Barbara Smith
Duncan Sousa

JOHNS HOPKINS UNIVERSITY SCHOOL OF MEDICINE
Baltimore, MD 21205-1503

Brian J. Eddie

U.S. NAVAL RESEARCH LABORATORY
Washington, DC 20375-0001

Kelley Betts

EXCET, INCORPORATED
Springfield, VA 22150-2519

FEBRUARY 2022

Disclaimer

The findings in this report are not to be construed as an official Department of the Army position unless so designated by other authorizing documents.

REPORT DOCUMENTATION PAGE

Form Approved
OMB No. 0704-0188

1. REPORT DATE *(DD-MM-YYYY)*	2. REPORT TYPE	3. DATES COVERED *(From - To)*
XX-02-2022	Final	Oct 2020 – Sep 2021

4. TITLE AND SUBTITLE
Purification and Characterization of a Membrane Sculpting Bacterial BAR Domain-Containing Protein for Engineering Tunable Scaffolds into Novel Biological Metamaterials

5a. CONTRACT NUMBER

5b. GRANT NUMBER

5c. PROGRAM ELEMENT NUMBER

6. AUTHOR(S)
Phillips, Daniel A. (ORISE); Miklos, Aleksandr E.; Buckley, Patricia E. (DEVCOM CBC); Lee, Jennifer A. (DTRA); Smith, Barbara; Sousa, Duncan (JHU); Eddie, Brian J. (NRL); Betts, Kelley (EXCET)

5d. PROJECT NUMBER
PE 0601102A Project VR9

5e. TASK NUMBER

5f. WORK UNIT NUMBER

7. PERFORMING ORGANIZATION NAME(S) AND ADDRESS(ES)
Director, DEVCOM CBC, ATTN: FCDD-CBR-BC, APG, MD 21010-5424
Oak Ridge Institute for Science and Education (ORISE); 1299 Bethel Valley Rd., Oak Ridge, TN 37830-8007
Defense Threat Reduction Agency; 8725 John J. Kingman Rd., MSC 6201, Fort Belvoir, VA 22060-6201
Johns Hopkins University School of Medicine; 855 N Wolfe St., Baltimore, MD 21205-1503
U.S. Naval Research Laboratory, Center for Bio/Molecular Science and Engineering; 4555 Overlook Ave. SW, Washington, DC 20375-0001
Excet, Inc.; 6225 Brandon Ave., Ste. 360, Springfield, VA 22150-2519

8. PERFORMING ORGANIZATION REPORT NUMBER
DEVCOM CBC-TR-1782

9. SPONSORING / MONITORING AGENCY NAME(S) AND ADDRESS(ES)
U.S. Army Surface Science Initiative Program, Combat Capabilities Development Command Chemical Biological Center; Aberdeen Proving Ground, MD 21010-5424

10. SPONSOR/MONITOR'S ACRONYM(S)
DEVCOM CBC

11. SPONSOR/MONITOR'S REPORT NUMBER(S)

12. DISTRIBUTION / AVAILABILITY STATEMENT
Approved for public release: distribution unlimited.

13. SUPPLEMENTARY NOTES

Metamaterial construction relies upon the ability to introduce precise features in surfaces at size scales proportional to the wavelength of the radiation being manipulated. Biology excels at forming precise structures on the nanometer to micrometer scale, but a fundamental understanding of the processes involved in their formation is essential to engineer these structures in a controlled manner. The ordered tubules formed through interaction between Bin/Amphiphysin/Rvs (BAR) domain-containing proteins and lipids fall within the diameter and length range required to affect visible light. A novel bacterial BAR domain-containing protein (BdpA) was investigated for its membrane sculpting capabilities both within the context of in vitro interaction between purified protein and liposomes and in vivo through protein expression and membrane extension formation. Predicted structures generated of BdpA show a characteristic BAR domain-like appearance and provide potential targets for engineering through targeted mutagenesis. Negative stain transmission electron microscopy experiments show that purified BdpA resembles previously characterized BAR domain proteins with intrinsic curvature and the predicted structure model. These initial experiments will serve to baseline future engineered membrane sculpting proteins towards the goal of using BAR domain protein-mediated tubule formation to generate tunable scaffolds for templating conductive structures, paving the way for biologically engineered metamaterials.

15. SUBJECT TERMS
Metamaterials; Synthetic biology; Membrane sculpting; Bin/Amphiphysin/Rvs (BAR) domain; Cell-free; Tunable; Obscurants

16. SECURITY CLASSIFICATION OF:			17. LIMITATION OF ABSTRACT	18. NUMBER OF PAGES	19a. NAME OF RESPONSIBLE PERSON
a. REPORT	b. ABSTRACT	c. THIS PAGE			Renu B. Rastogi
U	U	U	SAR	24	19b. TELEPHONE NUMBER *(include area code)* (410) 436-7545

Blank

PREFACE

The work described in this report was authorized under project number PE 0601102A Project VR9. The work was started in October 2020 and completed in September 2021.

The use of either trade or manufacturers' names in this report does not constitute an official endorsement of any commercial products. This report may not be cited for purposes of advertisement.

The text of this report is published as received and was not edited by the Technical Releases Office, U.S. Army Combat Capabilities Development Command Chemical Biological Center (DEVCOM CBC; Aberdeen Proving Ground, MD).

This report has been approved for public release.

Acknowledgments

The authors acknowledge the following individuals for their hard work and assistance with the execution of this technical program: Dr. Patricia McDaniel (DEVCOM CBC), Rebecca Braun, Jessica Parker, and Heather Rollyson (Booz Allen Hamilton; McLean, VA).

Blank

CONTENTS

1. INTRODUCTION 7

2. RESULTS 8

2.1 Expression and purification of BdpA 8
2.1.1. Expression tests in *Eschericia coli* 8
2.2 Predicted structure of BdpA 9
2.3 Transmission electron microscopy (TEM) of BdpA 10
2.3.1. Negative stain TEM of purified BdpA 10
2.3.2. *In vitro* tubule formation 11
2.4 Variation of *in vivo* BdpA membrane extension phenotypes 12

3. DISCUSSION 13

4. METHODS 14

4.1 Protein purification 14
4.2 *Ab initio* structure prediction 14
4.3 Liposome preparation 15
4.4 CFPS membrane sculpting assay 15
4.5 Negative stain TEM and *in vitro* tubule formation 15
4.6 *In vivo* BdpA expression and OME formation 16

5. ACKNOWLEDGMENTS 16

LITERATURE CITED 17

ACRONYMS AND ABBREVIATIONS 19

FIGURES

1. Expression tests of BdpA in *E. coli* cells. 9
2. Size exclusion chromatography of BdpA. 9
3. Predicted structure of BdpA. 10
4. Negative stain TEM of BdpA. 11
5. Demonstration of *in vitro* membrane sculpting activity of BdpA. 12
6. Membrane extension phenotypes *in vivo*. 13

PURIFICATION AND CHARACTERIZATION OF A MEMBRANE SCULPTING BACTERIAL BAR DOMAIN-CONTAINING PROTEIN FOR ENGINEERING TUNABLE SCAFFOLDS INTO NOVEL BIOLOGICAL METAMATERIALS

1. INTRODUCTION

Optical metamaterials (OMMs) impart a negative index of refraction, allowing electromagnetic fields to bend in unconventional directions.[1,2] OMMs are formed by patterning conductive structures into ordered, three-dimensional arrays on a surface such that the operational electromagnetic wavelength is larger than the spatial interval between the conductive materials.[3] The array of conductive materials creates surface plasmons, causing the incident electromagnetic waves to propagate parallel to the surface, rather than reflected back. This detail is very important for the long-term goal of optical cloaking technology and bending light around an object. For such materials to alter the way light reflects off a surface, a 3D structure must be within 10 to 100 nm in diameter,[3] making synthesis of OMMs that are functional within this range costly and difficult. Similarly, manufactured OMMs are bulky, cumbersome, and are seldom adaptable or responsive. In the context of developing a surface coating for the Warfighter at larger scales, these design constraints pose a significant challenge.

By contrast, biology excels at producing micro- and nanoscale ordered structures. Structural color occurs when non-pigmented but conductive biopolymers are ordered in the same 3D manner as man-made metamaterials. Visible light encounters the surface, but the precise ordering of the proteins creates a plasmonic effect, selectively reflecting a specific wavelength of light and producing color.[4,5] Examples of biological structures resulting in metamaterial-like properties (iridescence) can be found in bacterial colonies.[6] Bacterial cells can naturally form a self-healing coating on a surface, referred to as a biofilm. With the right components, bacterial synthesis offers a cost-effective and scalable method for the production of these types of materials.

Microscale lipid membrane features can also impart structural coloration on the macroscale, as evidenced by the brilliant blue color observed in the marble berry.[7,8] Forming lipids into precise structures requires the assistance of scaffolding or membrane sculpting proteins. In eukaryotic cells, membrane sculpting mechanisms are ubiquitous due to the necessity of membrane trafficking, organelle biogenesis, vesicle transport, and protein-lipid scaffolding.[9,10,11] The Bin/Amphiphysin/Rvs (BAR) domain family achieves membrane sculpting activity through electrostatic interactions between positively charged residues on the protein and negatively charged lipids, and the intrinsic curvature of certain members of the BAR domain family promote tubule formation through this protein-lipid association.[11] Recently, researchers coupled membrane sculpting (BAR) domain protein activity to light-actuated activity, resulting in controlled membrane deformation capabilities.[12] A bacterial membrane shaping BAR domain-like protein (BdpA) was identified in the conductive outer membrane extensions and vesicles produced naturally by *Shewanella oneidensis*. When expression of this protein is induced in cells, long-distance (>10 μm) outer membrane structures with a diameter less than 100 nm can be generated, posing a promising target for further characterization of biophysical activity and utilization through synthetic biology.

Here, we aim to solve the structure of this bacterial BAR domain protein and further characterize its membrane sculpting capabilities. This characterization will allow targeted mutagenesis of the protein towards the goal of altering the physical parameters of the resultant membrane tubules generated through protein-lipid interaction. The ability to alter dimensions and aspect ratios of membrane structures is an essential first step into producing tunable biological metamaterials from membrane scaffolds capable of performing over a range of electromagnetic wavelengths.

2. RESULTS

2.1 Expression and purification of BdpA

2.1.1. Expression tests in *Eschericia coli*

Heterologous expression of BdpA was tested in *E. coli* cells across a range of temperatures, inducer concentrations, and proprietary media optimized for protein expression. Isopropyl β-d-1-thiogalactopyranoside (IPTG) inducer concentration did not meaningfully affect soluble protein yield, but inducing cells overnight at 16 °C resulted in improved solubility (Figure 1a). The Western blot of the expression tests show no significant difference between inducer concentrations; therefore, the lowest inducer concentration of 50 μM IPTG was chosen moving forward. Out of each growth medium tested using the 16 °C overnight induction, Hyper broth yielded the highest concentration of soluble protein at the correct molecular weight of 56 kDa after immobilized metal ion chromatography (IMAC) purification (Figure 1c). Several other media formulations yielded similar (or higher) total protein yield after IMAC purification, but the elutions screened had less contaminating bands from the samples grown and induced in Hyper broth.

IMAC purification and size exclusion chromatography of codon-optimized BdpA
Following expression condition and construct codon optimization, BdpA was tested with an array of buffer additives to improve purification, protein stability, and monodispersity in solution (not shown). Here, size exclusion chromatography (SEC) highlights the results of this optimization, showing pure BdpA eluting from the SEC column. BdpA eluted in the first three peaks, suggesting that BdpA forms multimers in a similar manner to classic BAR domain-containing proteins.[13] The larger peak following the first three BdpA peaks was suspected to be Triton X-100 micelles, since a one percent solution of the detergent was used for purification, and Triton X-100 exhibits a strong absorbance at 280 nm.

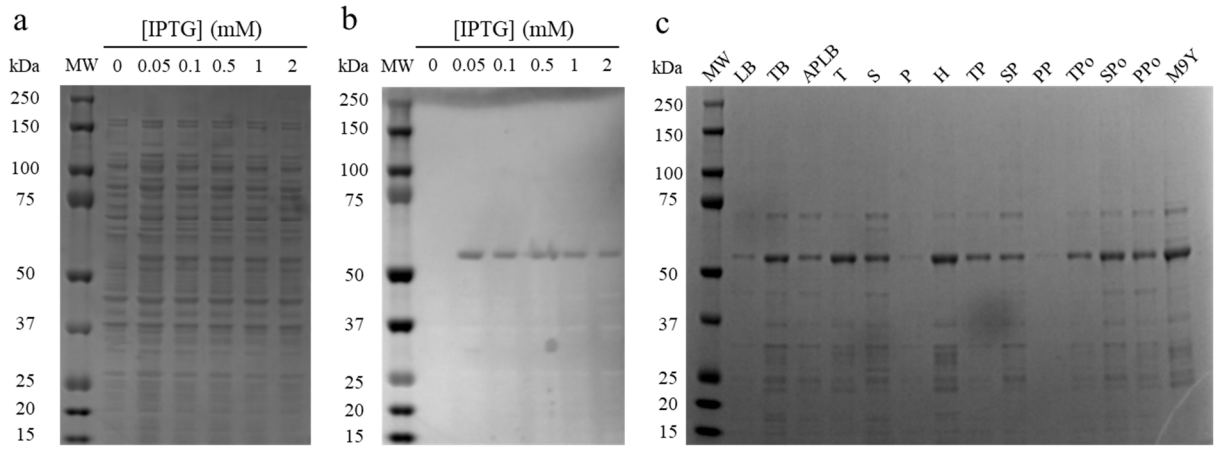

Figure 1. Expression tests of BdpA in *E. coli* cells.

a) SDS-PAGE of His-tagged BdpA expression (56 kDa) at indicated concentrations of IPTG. b) Western blot of the expression tests against the 6x-His tag. c) Expression and IMAC purification of His-tagged BdpA from cultures grown in different media. Luria-Bertani (LB), Teriffic Broth (TB), Animal Product-free LB (APLB), Turbo (T), Superior (S), Power (P), Hyper (H), Turbo Prime (TP), Superior Prime (SP), Power Prime (PP), Turbo Primeolate (TPo), Superior Primeolate (SPo), Power Primeolate (PPo), Glucose M9Y (M9Y).

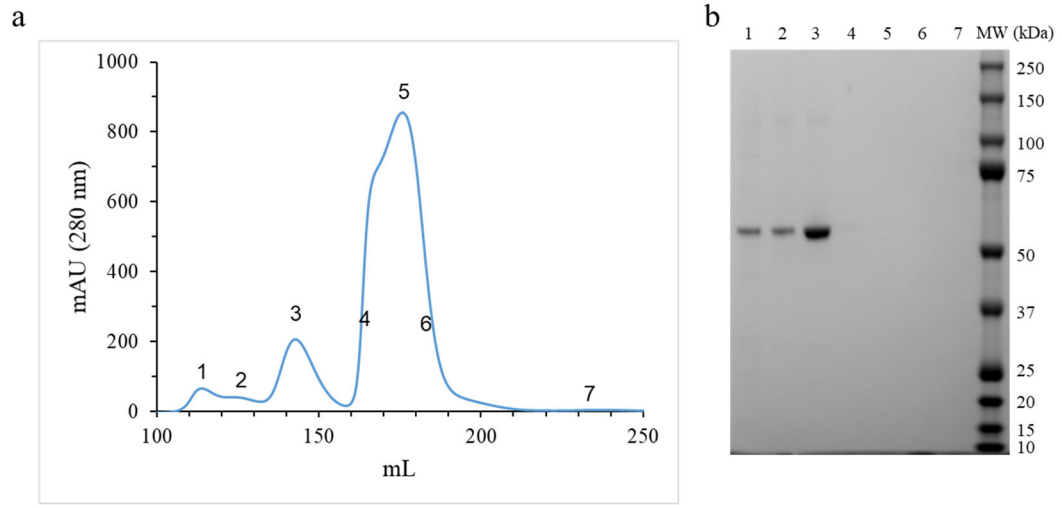

Figure 2. Size exclusion chromatography of BdpA.

a) Chromatogram of absorbance at 280 nm. b) SDS-PAGE of a fraction from the indicated peak numbers from the chromatogram. Peaks four, five, and six are Triton X-100.

2.2 Predicted structure of BdpA

In silico methods were employed to generate an *ab initio* predicted structure of BdpA in the absence of homology models. The predicted structure appeared as a jellyroll-like fold corresponding to the galactose-binding domain-like (GBD) region at the N-terminus of the protein, followed by a coiled coil in the predicted BAR domain section (Figure 3a). Homooligomerization models generated through trRosetta reveal a dimer with intrinsic "banana-shaped" curvature (Figure 3b), consistent with many other BAR domain-containing proteins.[13] The multisequence

alignment of BdpA homologs in other bacteria suggest variability and flexibility near the GBD, as well as within the dimerization interface of the coiled coils. We suspect that mutagenesis of the residues within these variability regions are promising targets for affecting membrane tubule diameter. Likewise, deletion of the specific protein domains could affect membrane sculpting functionality.

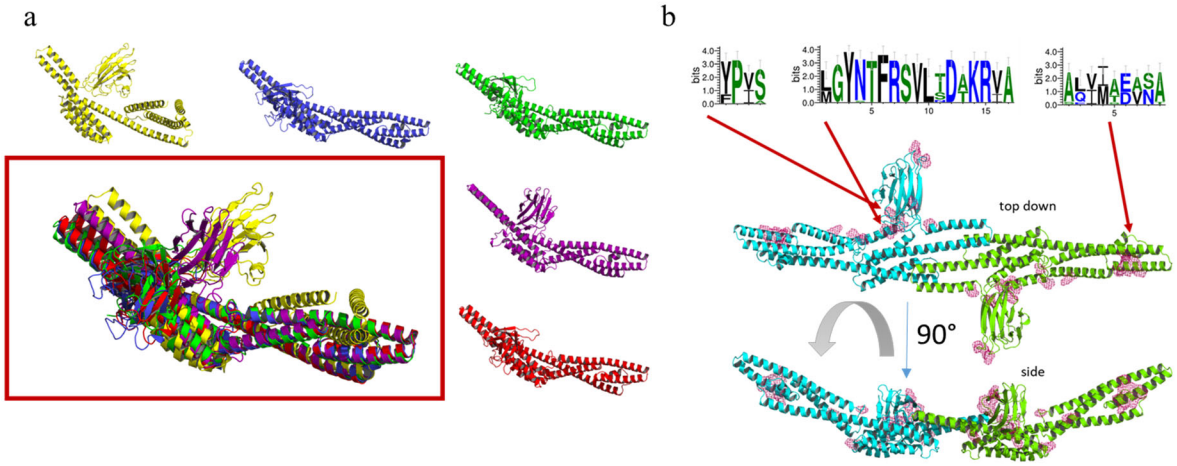

Figure 3. Predicted structure of BdpA.
a) Structure variability of the top 5 predicted models generated using trRosetta show flexibility in the GBD region. b) Predicted dimer from docking2 with sequence cartoons show the most frequent amino acid residues at each site highlighted in red on the dimer model.

2.3 Transmission electron microscopy (TEM) of BdpA

2.3.1. Negative stain TEM of purified BdpA

A solved structure of BdpA will provide valuable insight into how to engineer the protein through targeted mutagenesis. For structural analysis, the purified protein must be monodispersed on a grid such that individual particles can be analyzed. A dilution series of BdpA was prepared from a starting concentration of one mg/mL. A 1:100 dilution of the protein (10 µg/mL) provided the best particle dispersal on the grids and allowed the first glimpse at the protein structure. Here, "banana-like" dimers can be seen by TEM after negative staining (Figure 4).

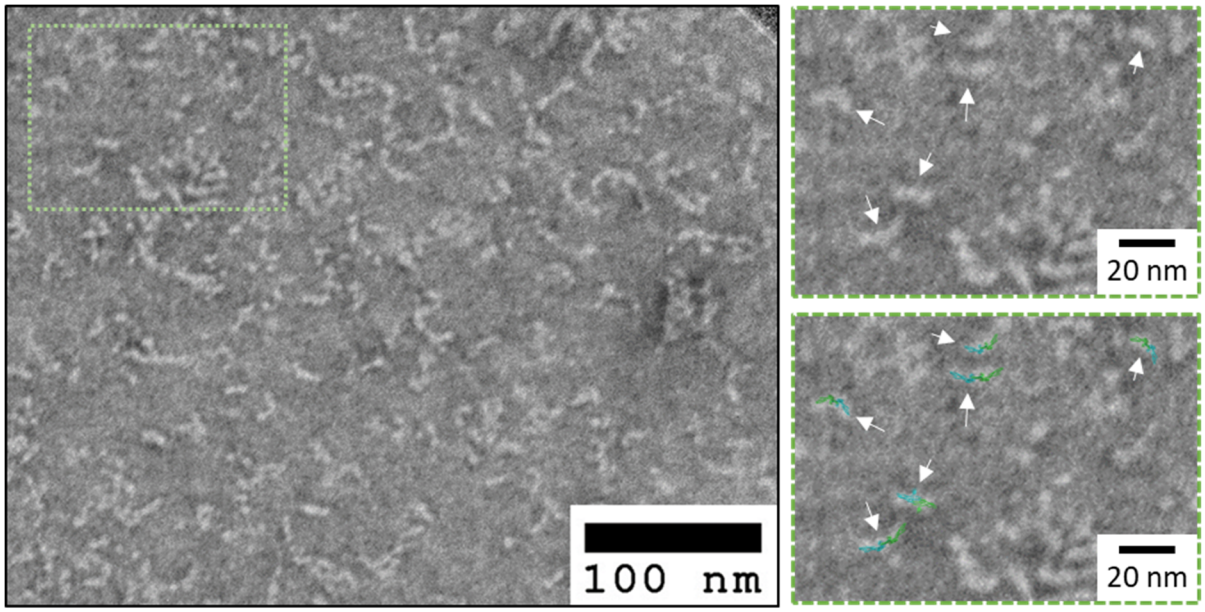

Figure 4. Negative stain TEM of BdpA.
Structures appear as coiled coils with BAR domain-like curvature showing similarity to the predicted structure from Figure 3. Enlarged inset image of the green box (top right) has white arrows pointing to BAR domain protein-like shapes, and bottom right inset shows these structures overlaid with the predicted dimer structure.

2.3.2. *In vitro* tubule formation

Lipid binding and curvature alteration are hallmarks of BAR domain protein activity. Through electrostatic interaction, purified BAR domain-containing proteins co-incubated with liposomes can form tubules.[9,10,11,13] Cell-free protein synthesis (CFPS) reactions offer a way to rapidly test protein expression and interaction in the absence of cells. To test *in vitro* tubule formation activity of BdpA, we engineered expression constructs comprised of the BAR domain-containing region alone (BdpA BAR only), BdpA without the cleavable signal peptide (BdpA no SP), and BdpA without the BAR domain region (BdpA GBD-like domain only). These constructs were expressed in CFPS reactions using a PURExpress reaction mix supplemented with liposomes prepared from the lipopolysaccharide (LPS) of *S. oneidensis* and labeled with the fluorescent, lipophilic dye FM 4-64 to visualize membrane structures. A network of tubule-like structures can be observed when the expression construct contained the BAR domain, but not in the GBD-only expression reaction nor the plasmid-free negative control (Figure 5a). This test demonstrated membrane curvature activity of the BAR domain region of BdpA, but higher resolution imaging is required to observe and measure the dimensions of the resultant tubule-like structures.

In vitro tubule formation assays of BAR domain proteins are typically performed by incubating purified protein with liposomes followed by imaging the reactions on grids using negative stain TEM. The presence of BdpA in the reactions resulted in tubules with a diameter less than 100 nm (Figure 5b). When the same samples were imaged by cryo-TEM, tubules were observed with BAR domain protein-like striations (Figure 5c).

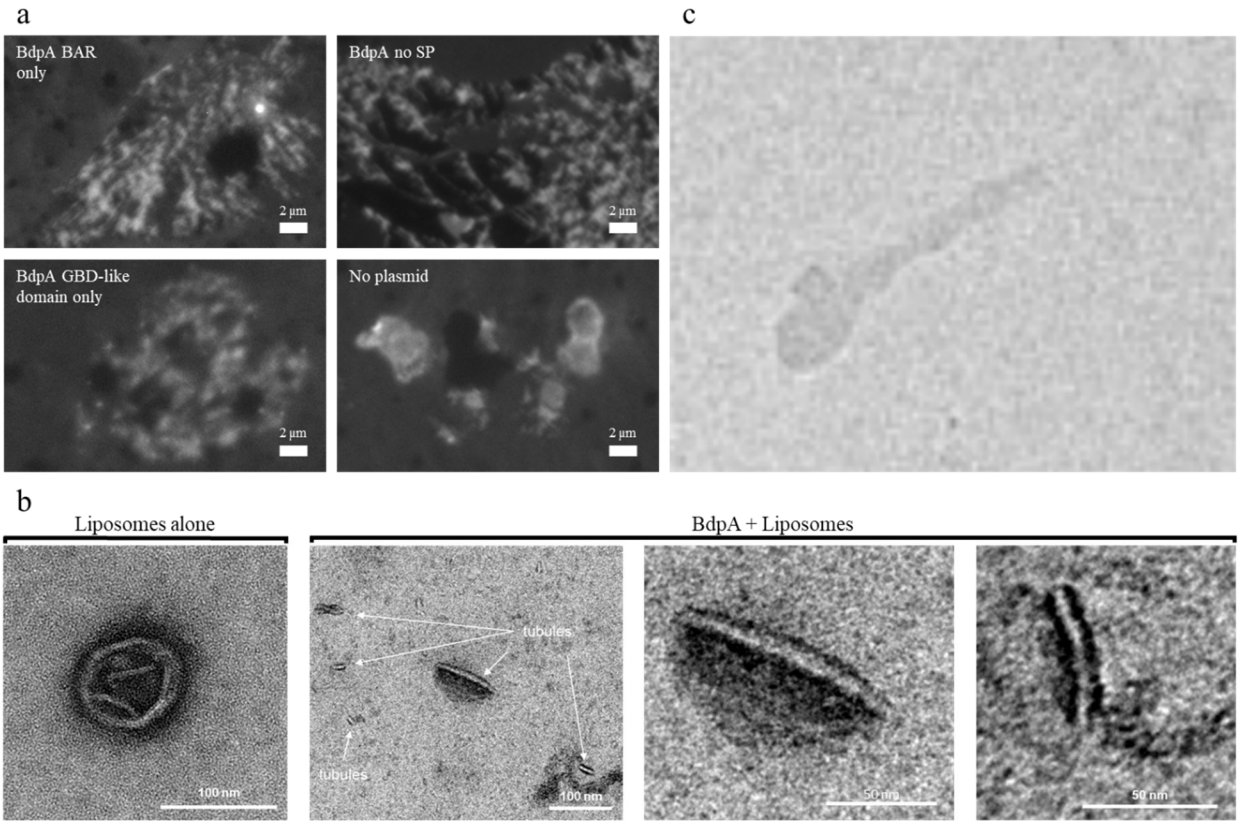

Figure 5. Demonstration of *in vitro* membrane sculpting activity of BdpA.
a) Fluorescence microscopy images of cell-free protein synthesis reactions using PURExpress with BdpA expression constructs and LPS-derived liposomes labeled with FM 4-64 lipophilic dye. b) Negative stain TEM images of *in vitro* tubule formation assays using either liposomes alone (left) or liposomes with purified BdpA (right). c) Cryo-TEM of *in vitro* tubule formation using BdpA and liposomes.

2.4 Variation of *in vivo* BdpA membrane extension phenotypes

When BdpA expression is induced in cells, membrane extensions are produced and can be visualized by fluorescence microscopy after addition of FM 4-64. We tested BdpA expression across a range of inducer concentrations and within different cell types to see if extension phenotypes would be affected. During induction in *E. coli* cells, phenotypes varied between outer membrane vesicles (OMVs), web-like outer membrane extensions (OMEs), or tubule-like OMEs (Figure 6). Inducer concentrations did not significantly alter the distribution of OME phenotypes (Figure 6b). However, expression of BdpA in different species revealed significant variation in the OME phenotypes between strains. *S. oneidensis* and *Marinobacter atlanticus* both exhibited more tubules, while *E. coli* produced predominately web-like OMEs (Figure 6c-e). We suspect the variation between strains is either due to the lipid composition of the LPS in the outer membrane or a consequence of a cell line engineered for heterologous overexpression of proteins.

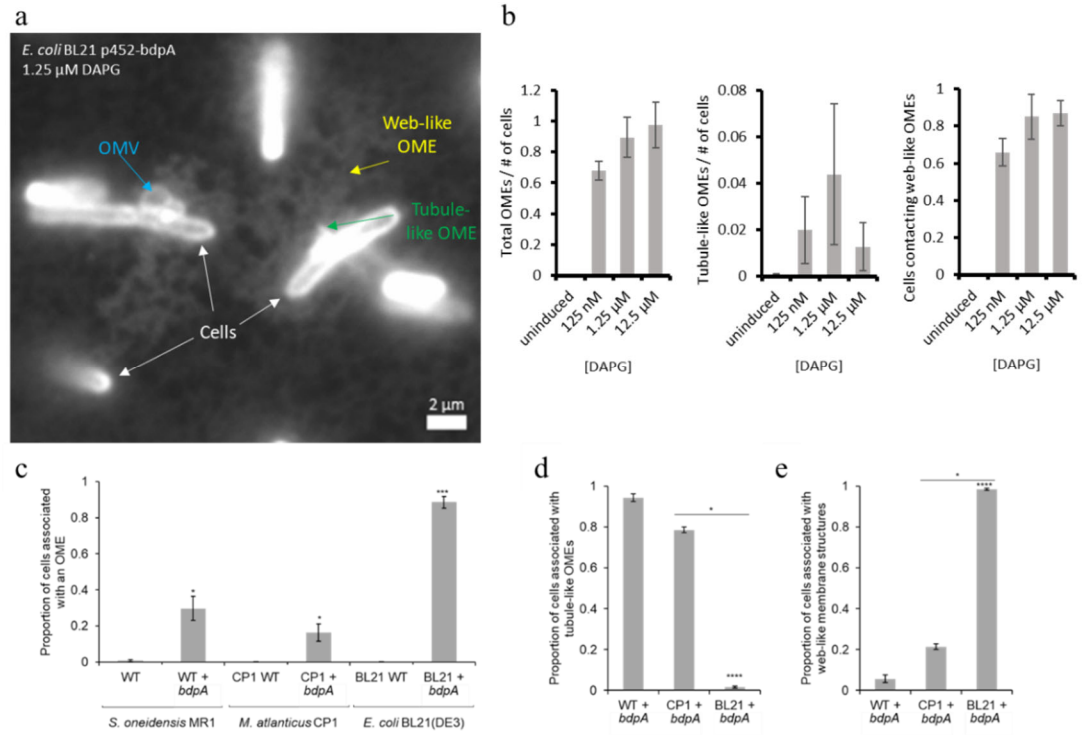

Figure 6. Membrane extension phenotypes *in vivo*.
a) Representative image of OME phenotypes produced upon induction of BdpA expression in cells labeled with FM 4-64. Scale = 2 µm. b) OME phenotypes observed from BdpA induction at varied concentrations of 2,4-diacetylphloroglucinol (DAPG) inducer in *E. coli* cells. c) Proportions of cells associated with an OME after induction of BdpA expression in *S. oneidensis* (WT), *M. atlanticus* (CP1), and *E. coli* (BL21). d) Proportion of cells associated with tubule-like OMEs, and e) associated with web-like OMEs between species following BdpA induction. Asterisks indicate statistical significance ($p < 0.05$, Welch's *t*-test).

3. DISCUSSION

Considerable evidence is mounting that BdpA is a functional, bacterial BAR domain protein. Protein purification and size exclusion chromatography revealed that BdpA is capable of forming oligomers with itself, and homodimerization is critical to eukaryotic BAR domain protein biophysical activity. Through preliminary TEM experiments, the purified protein was observed having a characteristic "banana-like" shape that was anticipated through *ab initio* structure prediction methods. Finally, the protein was capable of sculpting liposomes into tubules *in vitro* in a manner similar to other BAR domain-containing proteins. Future experiments will optimize the *in vitro* tubule formation conditions to improve tubule frequency and stability, and later iterations will include mutagenesis to alter the phenotype of the resultant membrane tubules.

Within the greater context of using these biological structures to template materials, we have provided a baseline for future protein engineering tests. Currently, the diameter of tubules produced *in vitro* is sufficient for a scaffold structure for templating conductive materials into metamaterials, but the length of the tubules is insufficient to provide the requisite aspect ratio.

Optimizing handling conditions to minimize shear forces could improve tubule length; similarly, an engineered BdpA protein that forms tighter, more stable oligomers could increase stability and tubule scaffold rigidity. Conversely, tubules resulting from BdpA expression in cells fit the length and diameter requirements, and biopolymer templating of extensions could be achieved through coexpression under the right conditions.

4. METHODS

4.1 Protein purification

BdpA constructs were ordered and cloned into the pET-28(a) expression vector with an N-terminal 6x-His tag, GSSGSS linker, and a thrombin cleavage site by Twist Bioscience. Plasmid constructs were transformed into chemically competent *E. coli* BL21(DE3) pLysS cells for protein expression. For protein expression, transformed cells were grown as overnight cultures in 30 mL Hyper broth (Athena ES) supplemented with 50 µM kanamycin and 25 µM chloramphenicol at 30 °C with 250 rpm shaking. Three cultures of 1 L Hyper broth with 50 µM kanamycin and 25 µM chloramphenicol were inoculated with 10 mL of the overnight culture and incubated at 37 °C with 250 rpm shaking until an OD_{600} of one was reached. Cultures were then cooled for 15 minutes in an ice bath, induced with 50 µM IPTG, and incubated overnight at 16 °C for 16 hours. Cultures were centrifuged, and the cell pellet was resuspended in 300 mL of lysis buffer (50 mM Tris, 500 mM NaCl, 40 mM imidazole, 1% Triton X-100, 1 mM DTT, 6 tablets of EDTA-free cOmplete protease inhibitor (Millipore Sigma), pH 8.0). Resuspended cells were lysed by microfluidization, centrifuged, and the clarified lysate was filtered through 0.45 µm filters before loading onto a 5 mL HisTrap Ni-NTA resin column on an AKTAxpress (Cytiva) FPLC machine. After loading, the column was washed with Buffer A (50 mM Tris, 500 mM NaCl, 40mM imidazole, 1% Triton X-100, 1 mM DTT, pH 8.0) until the A280 signal stabilized back to baseline. The imidazole gradient was increased to 80 mM until the A280 signal returned to baseline again. Finally, the imidazole concentration was ramped up to 500 mM, and fractions were collected of the purified protein. Fractions containing purified protein were dialyzed overnight into 4 L of 50 mM Tris, 500 mM NaCl, 0.1% Triton X-100, 1 mM DTT, pH8.0. Secondary purification size exclusion chromatography was performed by injecting 6 mL of the dialyzed elution onto a HiLoad Superdex S200 26/60 gel filtration column and collecting fractions. Fractions containing BdpA were determined by SDS-PAGE. These fractions were pooled, concentrated using a 30k MWCO spin concentrator, and the remaining Triton X-100 was desalted out using a HiTrap 5 mL Desalting column. Protein was diluted into 1 mg/mL aliquots and either used immediately or stored at 4 °C.

4.2 *Ab initio* structure prediction

A total of 278 BdpA homologs were identified across a range of bacterial species by BLAST. These homologs were used to build a multiple sequence alignment for ab initio structure prediction by trRosetta (Yang et al, 2020). Structures were visualized in the PyMOL Molecular Graphics System, Version 2.0 (Schrödinger, LLC). The BdpA dimer structure model was predicted using the RosettaDock and docking2 software on ROSIE (Lyskov and Gray, 2008; Chaudhury et al, 2011; Lyskov et al, 2013).

4.3 Liposome preparation

For CFPS membrane sculpting assays, LPS liposomes were made by rehydrating 0.5 mg of purified *S. oneidensis* LPS with 500 µL PURExpress *In Vitro* Protein Synthesis Kit (New England BioLabs) reaction mix, sonicating the lipid suspension at 30 °C for 10 minutes, then passing the sonicated mixture through 0.2 µm filters within a syringe liposome extruder 6 times (Avanti Polar Lipids). Liposome suspensions were prepared immediately prior to use, then labeled with FM 4-64 (ThermoFisher).

For negative stain TEM, LPS liposomes were prepared by rehydrating 1 mg of purified *S. oneidensis* LPS with 50 mM Tris, 250 mM NaCl, pH 8.0 buffer. Lipid suspensions were sonicated at 30 °C for 10 minutes, then passed through a series of sequentially smaller pored filters (1.0, 0.8, 0.4, and 0.2 µm) within a syringe liposome extruder 6 times per filter while incubating the extruder block at 30 °C.

4.4 CFPS membrane sculpting assay

Plasmids of protein constructs in the pET-28(a) vector were purified from glycerol stocks purchased from Twist Bioscience. All CFPS reactions were performed using the PURExpress reaction mix according to the manufacturer's specifications. Plasmids were diluted to 10 ng/µL, then 2 µL of each plasmid (or ddH_2O for plasmid-free control) were added to a separate 3 µL aliquot of the PURExpress reaction mixture. The plasmid reaction mix and the liposome reaction mix were combined in a 1:1 ratio in a total of 10 µL. Reactions were immediately transferred to a chambered cover glass slide and images were collected on a Zeiss LSM 800 confocal microscope with a Plan-Apochromat 63x/1.4 numerical aperture oil immersion M27 objective. Widefield fluorescence images were taken using a LED-Module 511 nm light source with 583-600 nm filters and a 91 He CFP/YFP/mCherry reflector. Excitation and emission spectra were 506 nm and 751 nm, respectively. Images were recorded using the Zeiss Zen software (Carl Zeiss Microscopy, LLC).

4.5 Negative stain TEM and *in vitro* tubule formation

Dilutions of 1 mg/mL purified BdpA were briefly incubated on copper grids. Samples (8 µL) were adsorbed to glow discharged (EMS GloQube) ultra-thin (UL) carbon coated 400 mesh copper grids (EMS CF400-Cu-UL), by floatation for 2 minutes. Grids were rinsed in three drops (one minute each) of buffer (50 mM Tris, 250 mM NaCl, pH 8.0) and negatively stained in two consecutive drops of 1% uranyl acetate (UA, aq.), and quickly aspirated. Grids were imaged on a Hitachi 7600 TEM operating at 80 kV with an AMT XR80 CCD (8 megapixel).

In vitro tubule formation assays were similarly performed as above with the following modifications. Purified BdpA was incubated with LPS liposomes at a 1:1 ratio of 0.1 mg/mL each. Samples were negatively stained in two consecutive drops of 0.75% uranyl formate (UF, aq.) and quickly aspirated. Grids were imaged on a Hitachi 7600 TEM operating at 80 kV with an AMT XR80 CCD (8 megapixel) or a Talos L120C with a Thermo-Fisher Ceta (cooled 16 Mpixel CMOS, 16-bit 1-25 fps).

For cryo-TEM of the *in vitro* tubule formation assays, samples were prepared as before, but were plunge frozen on grids into liquid ethane using a Vitrobot Mark IV System (Thermo Scientific). Images were taken using a Titan Krios cryo-TEM (Thermo Scientific).

4.6 *In vivo* BdpA expression and OME formation

To test for OME phenotypes resulting from BdpA induction in WT *S. oneidensis* (WT + *bdpA*), *M. atlanticus* (CP1 + *bdpA*), and *E. coli* (BL21 + *bdpA*), overnight cultures for each strain were diluted in LB for *S. oneidensis*, BB for *M. atlanticus*[14], or LB for *E. coli* to an OD_{600} of 0.05 and induced with the indicated concentration of DAPG for 1 hour at 30˚C (or 37˚C for *E. coli*) with 200 RPM shaking agitation. Prior to pipetting, ~1cm of the p200 pipette tip was trimmed to minimize shear forces during transfer. A 100 µL aliquot of each culture was labeled with 1 µL 1M FM 4-64, and 10 µl deposited onto chambered cover glass. Each sample was imaged immediately after deposition onto the glass slides.

Imaging experiments were performed on at least 3 individual biological replicate experiments per strain, and are representative images from 5-10 fields of view per replicate from 700 cells for *S. oneidensis* WT, 472 cells for *S. oneidensis* WT + *bdpA*, 4041 cells for *M. atlanticus* CP1 WT, 150 cells for *M. atlanticus* CP1 + *bdpA*, 2190 cells for *E. coli* BL21 WT, and 2623 cells for *E. coli* BL21 + *bdpA*. The proportion of cells producing either type of membrane feature was calculated by dividing the number of cells for which a membrane feature was observed by the number of total cells for each strain; the proportions from each independent experiment were averaged for each strain to obtain the mean proportions for each strain that were plotted in bar graphs. The proportion of cells associating with OMEs observed from each biological replicate culture was recorded, as well as if the associated OME resembled either a tubule-like or web-like structure. Tubule-like OMEs were defined as narrow, unbranching membrane extensions. Cells that were associated with a branching, reticular membrane were counted as producing a web-like OME. Statistical significance of the proportions of cells associated to each of the OME phenotypes between strains was determined by Welch's *t*-test.

5. ACKNOWLEDGMENTS

We would like to thank Robert Ernst at the University of Maryland, Baltimore for preparing the purified LPS used in this study, and Brian Eddie for his technical help counting membrane extensions. We especially thank Katherine Rhea for the intellectual conversations about troubleshooting and training on specific equipment. Daniel Phillips and Aleksandr Miklos wrote the proposal, acquired funding, planned and supervised research, generated predicted structure models, and wrote the report. Daniel Phillips and Jennifer Lee purified proteins. Jennifer Lee performed expression and buffer additive testing, as well as intellectual discussions. Barbara Smith and Duncan Sousa performed TEM experiments. Daniel Phillips, Jennifer Lee, and Aleksandr Miklos interpreted data. Funding was provided by the U.S. Army via the Surface Science Initiative Program (PE 0601102A Project VR9) at the Combat Capabilities Development Command Chemical Biological Center.

LITERATURE CITED

[1] Pendry, J.B.; Smith, D.R.. Reversing Light With Negative Refraction. *Physics Today*, **2004**, 57 (6), p. 37-43.

[2] Pendry, J.B.; Schurig, D.; Smith, D.R. Controlling electromagnetic fields. *Science*, **2006**. 312 (5781), p. 1780-2.

[3] DuFort, C.C.; Dragnea, B. Bio-enabled synthesis of metamaterials. *Annu. Rev. Phys. Chem.*, **2010**. 61, p. 323-44.

[4] Ruiz-Clavijo, A.; Tsurimaki, Y.; Caballero-Calero, O.; Ni, G.; Chen, G.; Boriskina, S.V.; Martín-González, M. Engineering a full gamut of structural colors in all-dielectric mesoporous network metamaterials. *ACS Photonics*, **2018**. 5 (6), 2120-2128.

[5] Yang, W.; Xiao, S.; Song, Q.; Liu, Y.; Wu, Y.; Wang, S.; Yu, J.; Han, J.; Tsai, D. All-dielectric metasurface for high performance structural color. *Nat. Commun.*, **2020**. 11, 1864.

[6] Johansen, V.; Catón, L.; Hamidjaja, R.; Oosterink, E.; Wilts, B.; Rasmussen, T.; Sherlock, M.; Ingham, C.; Vignolini, S. Genetic manipulation of living bacterial color. *Proc. Natl. Acad. Sci.*, **2018**. 115 (11), p. 2652-2657.

[7] Vignolini, S.; Rudall, P.; Rowland, A.; Reed, A.; Moyroud, E.; Faden, R.; Baumberg, J.; Glover, B.; Steiner, U. Pointillist structural color in Pollia fruit. *Proc. Natl. Acad. Sci.*, **2012**. 109 (39), p. 15712-15715.

[8] Middleton, R.; Sinnott-Armstrong, M.; Ogawa, Y.; Jacucci, G.; Moyroud, E.; Rudall, P.; Prychid, C.; Conejero, M.; Glover, B.; Donoghue, M.; Vignolini, S. Viburnum tinus fruits use lipids to produce metallic blue structural color. *Cell Current Biology*, **2020**. (30), p. 3804-3810.

[9] Daum, B.; Auerswald, A.; Gruber, T.; Hause, G.; Balbach, J.; Kühlbrandt, W.; Meister, A. Supramolecular organization of the human N-BAR domain in shaping the sarcolemma membrane. *J. Struc. Bio.*, **2016**. 194, p. 375-382.

[10] Daumke, O.; Roux, A.; Haucke, V. BAR domain scaffolds in dynamin-mediated membrane fission. *Cell*, **2014**. 156 (5), p. 882-892.

[11] Frost, A.; Perera, R.; Roux, A.; Spasov, K.; Destaing, O.; Egelman, E.H.; De Camilli, P.; Unger, V.M. Structural basis of membrane invagination by F-BAR domains. *Cell*, **2008**. 132 (5), p. 807-817.

[12] Jones, T.; Liu, A.; Cui, B. Light-inducible generation of membrane curvature in live cells with engineered BAR domain proteins. *ACS Syn. Bio.*, **2020**. 9 (4), p. 893-901.

[13] Simunovic, M.; Evergren, E.; Callan-Jones, A.; Bassereau, P. Curving cells inside and out: roles of BAR domain proteins in membrane shaping and its cellular implications. *Annu. Rev. Cell Dev. Bio.*, **2019**. 35 (1), 111-129.

[14] Bird, L.; Wang, Z.; Malanoski, A.; Onderko, E.; Johnson, B.; Moore, M.; Phillips, D.; Chu, B.; Doyle, J.; Eddie, B.; Glaven, S. Development of a genetic system for Marinobacter atlanticus CP1 (sp. nov.), a wax ester producing strain isolated from an autotrophic biocathode. *Front Microbiol.*, **2018**. (9), p. 3176.

Blank

ACRONYMS AND ABBREVIATIONS

BAR	Bin/Amphiphysin/Rvs
BdpA	BAR domain-like protein
CFPS	Cell-free protein synthesis
GBD	galactose-binding domain-like
IMAC	immobilized metal ion chromatography
IPTG	Isopropyl β-d-1-thiogalactopyranoside
LPS	lipopolysaccharide
OMEs	outer membrane extensions
OMMs	Optical metamaterials
OMVs	outer membrane vesicles
SEC	size exclusion chromatography
TEM	Transmission electron microscopy

Blank

DISTRIBUTION LIST

The following individuals and organizations were provided with one Adobe portable document format (pdf) electronic version of this report:

U.S. Army Combat Capabilities Development Command Chemical Biological Center (DEVCOM CBC)
BioSciences Division
FCDD-CBR-BC
ATTN: Phillips, D.
Miklos, A.
Buckley, P.
FCDD-CBR-B
ATTN: Rosenzweig, N.
FCDD-CBR
ATTN: McDaniel, P.

DEVCOM CBC Technical Library
FCDD-CBR-L
ATTN: Foppiano, S.
Stein, J.

Defense Threat Reduction Agency
RD-CBR
ATTN: Jensen, N.

Defense Technical Information Center
ATTN: DTIC OA

U.S. ARMY COMBAT CAPABILITIES DEVELOPMENT COMMAND
CHEMICAL BIOLOGICAL CENTER